Free-Running Droplets

Fabrice Domingues Dos Santos and Thierry Ondarçuhu
Laboratoire de Physique de la Matière Condensée (U.A. CNRS 792), Collège de France, 11 Place Marcelin Berthelot, 75231 Paris Cedex 05, France
(Received 10 July 1995)

We present a detailed study of an original spreading behavior observed with nonvolatile droplets containing surface-active agents: The droplet moves spontaneously on the surface with velocities on the order of a few centimeters per second. For small droplets, this self-supported motion may be interpreted in terms of capillary models, which gives precise information about the reaction mechanism that occurs at the surface. For large droplets, gravity intervenes and we observed an important change in the profile of the droplets and different spreading regimes.

PACS numbers: 68.45.–v, 47.70.Fw

The spreading of liquid droplets on solid surfaces plays a critical role in numerous technological processes. The early works on classical capillarity have been extended recently to give a precise description of the wetting of ideal surfaces by both nonvolatile [1,2] and volatile liquids [3]. The situations encountered in practice are, however, much more complex, because the heterogeneities of the surface lead to important hysteresis phenomena. We have been investigating previously the properties of simple heterogeneous surfaces: a model system called "mixed surfaces" consisting of two regions of different wettabilities, one hydrophilic denoted as P (for polar), and one hydrophobic denoted as A (for apolar). These surfaces exhibit particular wetting properties; in particular, a droplet deposited on the boundary between P and A moves spontaneously towards the P part [4] (except if the liquid completely wets the two solids giving a film at equilibrium on the boundary [5]). This effect can be understood by considering that small spherical droplets are not at equilibrium as they are subjected to noncompensated Young forces directed towards the P part [see Fig. 1(a)]. Starting from this observation, we imagined a situation where the liquid would be able to modify a hydrophilic surface, by some reactive mechanism that renders it hydrophobic. The droplet would then always be out of equilibrium between the hydrophilic bare substrate it meets at the front and the hydrophobic trail it leaves behind, as schematized in Fig. 1(b). One would therefore expect the droplet to move continuously on the surface, leading to "free-running droplet."

In order to test this idea experimentally, we used droplets of n-alkanes (n-octane and n-dodecane) containing 1H,1H,2H,2H-perfluorodecyltrichlorosilane, because the silane molecules can form dense grafted monolayers on silicon or glass and are used to render these surfaces hydrophobic [6]. When we deposited such a droplet on a glass surface and initiated a motion by pushing it with a pipette, we observed that it continued to move on the substrate, as expected. This self-supporting movement ended only when the droplet had no more hydrophilic surface available (we never observed a limitation due to silane depletion) and was observed even on inclined substrates on which the droplet ran uphill. On a horizontal surface, the trajectory was quite erratic, because the silanization reaction is very sensitive to any chemical heterogeneity of the substrate. Notice that a droplet cannot cross the hydrophobic trail left by itself or another droplet. This self-avoiding motion is illustrated in Fig. 2, where the trajectories of two droplets are revealed by a breath figure. In order to obtain reproducible and quantitative effects, we took advantage of the fact that a droplet avoids hydrophobic surfaces to guide it on a rectilinear track. We used the techniques of forming mixed surfaces [4] to prepare glass surfaces that are hydrophobic everywhere except on a linear strip. The movement of a reactive droplet is thus

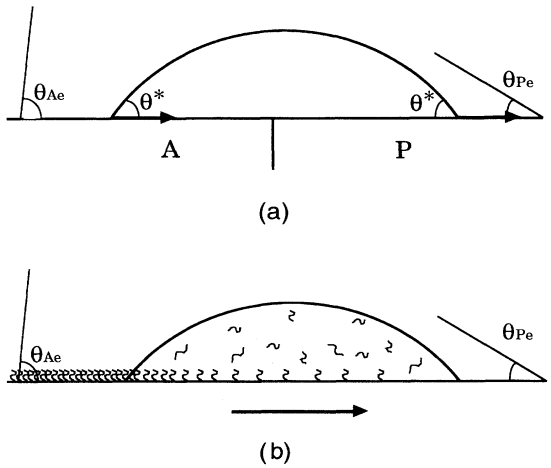

FIG. 1. (a) Schematic representation of a droplet deposited on the boundary between the two parts A and P of a mixed surface. θ_{Ae} and θ_{Pe} are the equilibrium contact angles on A and P, respectively, and θ^* is the dynamical contact angle of the droplet. The arrows depict the resultant of the Young forces that occur on each contact line. (b) Schematic representation of a free-running droplet. The silanes in solution graft on the surface to give a hydrophobic surface characterized by the contact angle θ_{Ae} that depends on the surface coverage ϕ_s.

 0031-9007/95/75(16)/2972(4)$06.00

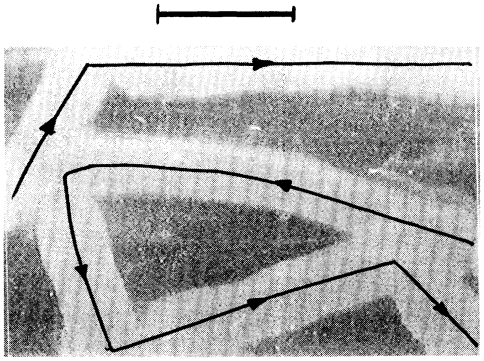

FIG. 2. Breath figure on a glass slide crossed by two free-running droplets. Water vapor condenses differently on the hydrophilic and hydrophobic parts and reveals the trail left by the droplets. The arrows represent the direction of motion. We note that the trajectories cannot cross. Upper and lower limits of the picture are the edges of the glass slide. The bar corresponds to 1 cm.

confined to the hydrophilic track (Fig. 3). The cleaning of the samples is also a crucial condition to obtain reproducible measurements, because silanization is sensitive to contamination of the surface. Before forming the mixed surface, the samples were cleaned with sulfochromic acid and then rinsed with copious amounts of water; this last point is very important, because a physisorbed layer of water is needed to obtain good reaction of the silane with the surface [7]. The motion of the droplet was then videotaped using a CCD camera with a $\frac{1}{1000}$ s shutter in order to obtain sharp images. The positions of the droplet and the dynamic contact angle were measured using an image processing software.

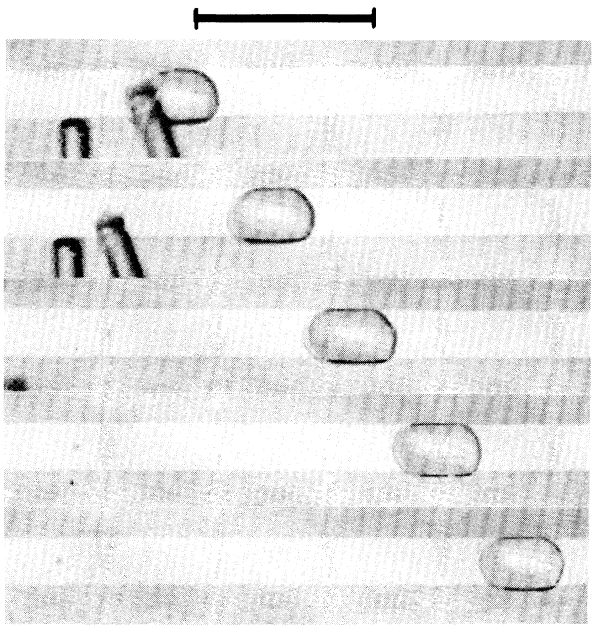

FIG. 3. Top views of a free-running droplet guided on a track delimited by hydrophobic regions. The time interval between two pictures is 0.1 s and the bar corresponds to 1 cm. In order to visualize the track, we put the glass slide on a sheet of paper with shaded regions corresponding to the approximate location of the hydrophobic parts. The dark object appearing in the top two panels is the pipette used to deposit the liquid (and its image by reflection on the glass).

We first consider droplets with a length smaller than $\kappa^{-1} = (\gamma/\rho g)^{1/2}$, the capillary length, which is a few mm for our experimental conditions (γ is the surface tension of the liquid; ρ is its density). At this scale, gravitational effects can be neglected. The pressure in the liquid being uniform, the droplets have circular profiles as schematized in Fig. 1. By plotting the evolution of the rear and front line positions of small moving droplets, we observed that the droplets moved with constant velocity V and constant length L. By changing the relevant parameters of the system (liquid viscosity, silane concentration, droplet volume), we were able to explore a large range of velocities (from 1 mm/s to 10 cm/s). In Fig. 4 we plot the velocity of octane droplets of a given volume against the concentration in reactive agents. We observe that the velocity first increases rapidly and then reaches a saturation level at high concentrations. When we plot the evolution of the velocity against the length of the droplet for two different concentrations in silane, we notice the same kind of behavior (Fig. 5). These results clearly show that the velocity is related to the quality of the grafted layer left by the droplet: The higher the concentration of reactive agents in the solution, the denser the grafted layer; the larger the droplet, the longer the reactive agents can graft onto a site on the substrate. To characterize the quality of the grafted layer, we measured the equilibrium contact angle of pure alkane on the hydrophobic trail. A dense layer gives a very hydrophobic surface and consequently

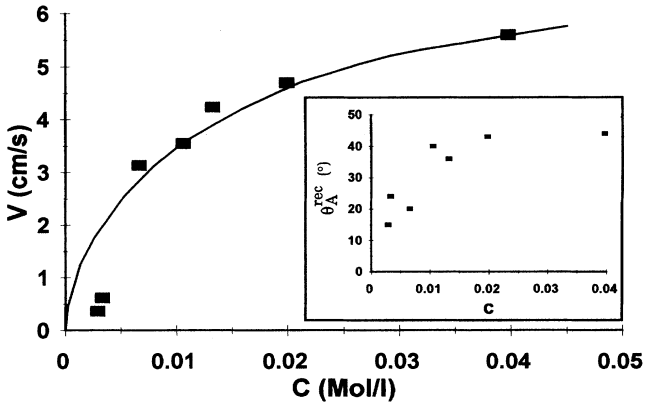

FIG. 4. Plot of the velocity of octane droplets of length $L = 3.5$ mm as a function of the concentration in silane. The solid curve corresponds to the result of solving Eqs. (1)–(4). Inset: Receding contact angle of pure octane measured on the hydrophobic trail left by the same droplets.

a large equilibrium contact angle. In practice, on real surfaces, we do not measure an equilibrium angle, because hysteresis (often several degrees) is observed between the advancing contact angle θ_A^{adv} and the receding one θ_A^{rec}. According to Ref. [4], the relevant angle in our case is θ_A^{rec}. In Fig. 4 we show the evolution of θ_A^{rec} with concentration. As with velocity, we observe a large range of contact angles, a rapid increase, and a saturation level around 46°, which corresponds to the receding contact angle measured on a dense grafted layer obtained from a silanization bath. These observations led us to plot velocities of all droplets with different lengths and concentrations in reactive agents against the variable θ_A^{rec}. All of the points fell on the same curve. Examples of such curves are shown in Fig. 6 for octane and dodecane which differ mainly by their viscosity. Note also that these data give an estimate of the reaction time, which is on the order of the time a site of the substrate is in contact with the liquid (i.e., $L/V \approx 0.1$ s). This observation indicates that silanization is very rapid.

In order to interpret our results, we used first the model developed for mixed surfaces [8]—that is, we took into account the difference in wettability, without considering the reaction mechanism. The theoretical analysis of Raphaël, in the case of ideal surfaces, shows that the droplet reaches a constant velocity given by

$$V = \frac{\gamma}{6l\eta} \tan\theta^* (\cos\theta_{Pe} - \cos\theta_{Ae}), \qquad (1)$$

where γ is the surface tension of the liquid, η is its viscosity, l is a logarithmic factor ($l = \ln x_{\max}/x_{\min}$, the ratio of macroscopic and molecular lengths), and θ^* is the dynamic contact angle:

$$2\cos\theta^* = \cos\theta_{Ae} + \cos\theta_{Pe}. \qquad (2)$$

Note that, as demonstrated in Ref. [4], expressions (1) and (2) can be used for a real surface with hysteresis by replacing θ_{Pe} and θ_{Ae} by θ_P^{adv} and θ_A^{rec}, respectively.

Expressions (1) and (2) can be applied to the case of free-running droplets, because they give the dependency of the velocity on the equilibrium contact angle θ_A^{rec}. The values of η, γ, and θ_P^{adv} are measured experimentally and l was used as an adjustable parameter. As shown in Fig. 6, the theoretical curves fit the experimental results well for the two different systems, using a unique value of the parameter l. The value $l = 20$ is compatible with the one deduced from other different experiments [4,9]. Moreover, on the images, we verified that the dynamical contact angle is in agreement with Eq. (2). These results validate that view of free-running droplets as being continuously out of equilibrium on a mixed surface.

The previous model interprets the velocities measured with a phenomenological parameter θ_A^{rec}. Recently, Brochard and de Gennes [10] went a step further by taking into account the reaction mechanism. They assumed that the equilibrium contact angle obtained on the hydrophobic trail depends on the surface coverage ϕ_s (fraction of the surface sites that have been functionalized after the droplet has passed) by the relation

$$\gamma\cos\theta_{Ae} = \gamma\cos\theta_{Pe} - \gamma_1\phi_s, \qquad (3)$$

where γ_1 is a constant that can be determined experimentally. Assuming that the silanization reaction follows first-order kinetics, they deduced the following rate equation for the surface coverage ϕ_s:

$$\phi_s = 1 - \exp\left(-\frac{t}{\tau}\right) = 1 - \exp\left(\frac{L}{V\tau}\right) \text{ with } \frac{1}{\tau} = kc, \qquad (4)$$

where k is the rate constant, c is the silane concentration in the droplet, and τ is the time constant of the reaction. By coupling Eqs. (1)–(4) one can obtain a relation between L, V, and c. Assuming a weak dependence of θ^* on the velocity V, Brochard and de Gennes obtained an analytical expression

$$L = V\tau\ln\left(\frac{V_1}{V_1 - V}\right) \text{ with } V_1 = \frac{\gamma_1\theta^*}{6l} \qquad (5)$$

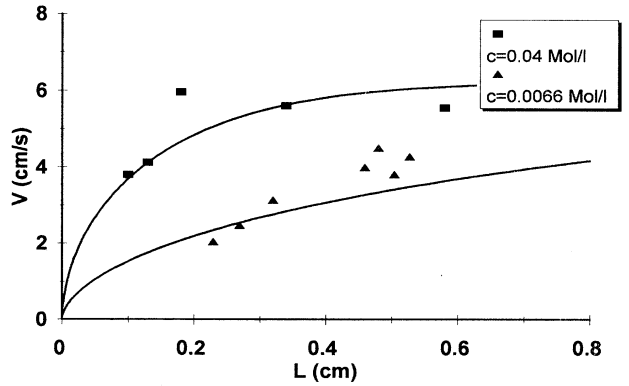

FIG. 5. Plot of the velocity of octane droplets as a function of their length for two different concentrations of silane. The solid curves correspond to the result of solving Eqs. (1)–(4).

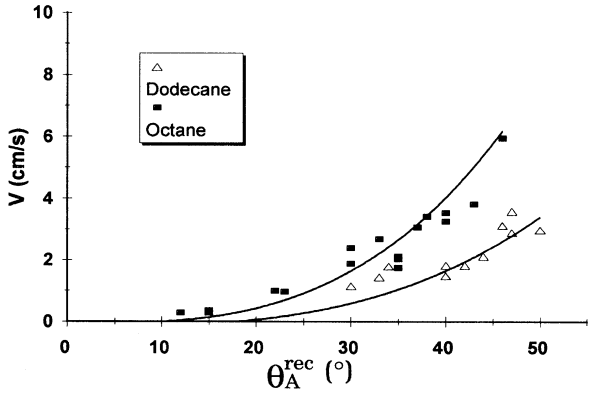

FIG. 6. Curves obtained by plotting the velocities of droplets of different sizes and concentrations as a function of the contact angle measured on the trail, for toctane and dodecane. Solid curves correspond to Eq. (1).

FIG. 7. Photograph of the profile of a large droplet (L = 1.2 cm). The picture is symmetric because of the reflection of the image on the substrate. The arrow indicates the direction of motion.

that accounts for the saturation of the curves $V(L)$ and $V(c)$ for a value of the velocity V_1. In our experiments, however, since the dynamic contact angle θ^* varied between 12° and 35° and could not be considered as a constant, we could not directly use expression (5).

In order to compare the model with the experimental data, we solved Eqs. (1)–(4) by numerical methods. Using Eq. (3), we determined experimentally the value of γ_1 considering that the maximum contact angle measured corresponds to the limit $\phi_s = 1$ of a compact layer. Thus, the only unknown quantity was k, the rate constant of the reaction, which we used as an adjustable parameter. With a single value $k = 1100\ \mathrm{s}^{-1}\,\mathrm{mol}^{-1}\,\mathrm{l}$, we were able to fit all of the $V(c)$ and $V(L)$ curves as shown in Figs. 4 and 5; this validates the assumption of first-order kinetics for the silanization. The time constant τ is therefore inversely proportional to the concentration of silane molecules in the droplet. Notice that the silanization is a very rapid process as, for the concentrations used, τ varies from 0.01 to 0.2 s. It is worth noting that this model gives a prediction of the velocity of a droplet as a function of its size and concentration of silane, which was not provided by the previous model [Eqs. (1) and (2)].

We now consider the case of large droplets. When the droplet is larger than the capillary length, gravity effects are no longer negligible and induce dramatic changes in the profile of the droplets [11]. It is well known that large, static droplets are flattened to a thickness that depends on the equilibrium contact angle. In the case of free-running droplets larger than 1 cm, we observed (Fig. 7) that the droplet was flattened and asymmetric. The difference between the contact angle at the front and that at the rear induces a dissymmetry in the profile and a slope in the central region. Moreover, experimental measurements show that for the same equilibrium contact angle on the trail, an asymmetric droplet moves faster than a symmetric one. For such droplets, the capillary model can no longer be applied. It has been shown by Brochard [12] that in the case of large droplets an additional driving force has to be considered. This force is due to the horizontal pressure gradient induced by the slope of the central region. This leads to the following expression of the velocity:

$$V = 2\frac{\rho g}{3\eta}\kappa^{-1}\,\frac{\sin(\theta_{Ae}/2) - \sin(\theta_{Pe}/2)}{L}\,h_0^2, \qquad (6)$$

where h_0 is the mean height of the droplet. This expression accounts for the increase in velocity induced by gravity, but the calculation gives values larger than those obtained experimentally. In fact, this model was derived in the case of a small difference in wettability: Velocities should be small and the contact angles should be close to the equilibrium values. This is not the case in our experiments, where the velocities were large. We solved the problem numerically by replacing in Eq. (6) θ_{Pe} and θ_{Ae} by the dynamical contact angles $\theta_P(V)$ and $\theta_A(V)$ obtained by hydrodynamic analysis [1]. We found, in the case of octane, velocities of about 7 cm/s, in good agreement with the experimental values. This model also predicts a decrease in the velocity with the length of the droplet. This effect is weak and would require very large droplets to be observed experimentally. When we increased the size of the droplets with high concentrations of silane, the motion was, however, no longer a uniform translation: We observed a periodic oscillation in the length and velocity of the droplet. This effect remains to be understood, probably by taking into account inertial effects.

To summarize, we have presented a quantitative study of the spontaneous translation of reactive droplets that modify the wettability of the substrate on which they are moving. Under controlled and reproducible conditions, we observed a large range of velocities going from 1 mm s^{-1} to 10 cm s^{-1}. In the case of small droplets, the results are well explained in terms of a model combining a capillary approach and the kinetics of the chemical reaction that occurs at the surface. In the case of droplets larger than the capillary length, we showed new regimes that require further investigations, which are currently under way.

We thank E. Raphaël, F. Brochard, P. G. de Gennes, and M. Veyssié for fruitful discussions.

[1] P. G. De Gennes, Rev. Mod. Phys. **57**, 827 (1985).
[2] L. Léger and J. F. Joanny, Rep. Prog. Phys. **55**, 431 (1992).
[3] S. Dietrich, in *Phase Transitions and Critical Phenomona,* edited by C. Domb and J. L. Lebowitz (Academic, London, 1988), Vol. 12, p. 1.
[4] T. Ondarçuhu and M. Veyssié, J. Phys. II (France) **1**, 75 (1991).
[5] W. Koch, S. Dietrich, and M. Napiorkowski, Phys. Rev. E **51**, 3300 (1995).
[6] J. B. Brzoska, N. Shahidzadeh, and F. Rondelez, Nature (London) **360**, 719 (1992).
[7] P. Silberzan, L. Léger, D. Ausserré, and J. J. Benattar, Langmuir **7**, 1647 (1991).
[8] E. Raphaël, C. R. Acad. Sci. Paris **306**, 751 (1988).
[9] T. Ondarçuhu and M. Veyssié, Nature (London) **352**, 418 (1991).
[10] F. Brochard and P. G. de Gennes (to be published).
[11] C. Redon, F. Brochard-Wyart, H. Hervet, and F. Rondelez, J. Colloid Interface Sci. **149**, 580 (1992).
[12] F. Brochard, Langmuir **5**, 432 (1989).

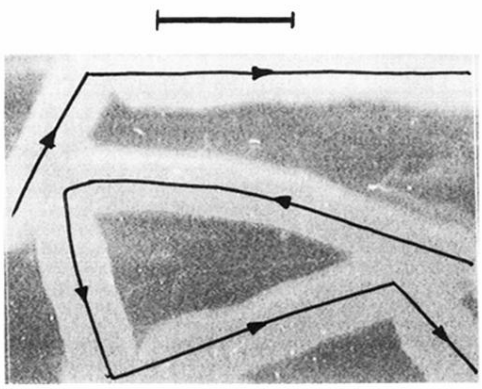

FIG. 2. Breath figure on a glass slide crossed by two free-running droplets. Water vapor condenses differently on the hydrophilic and hydrophobic parts and reveals the trail left by the droplets. The arrows represent the direction of motion. We note that the trajectories cannot cross. Upper and lower limits of the picture are the edges of the glass slide. The bar corresponds to 1 cm.

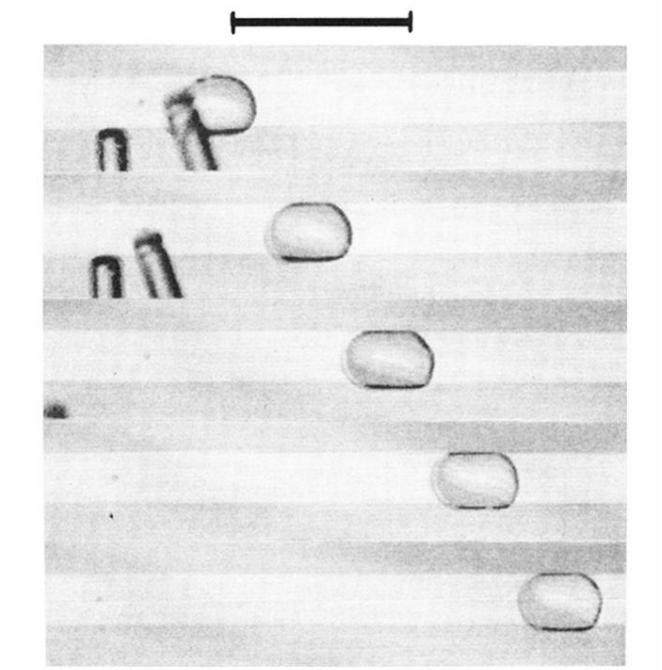

FIG. 3. Top views of a free-running droplet guided on a track delimited by hydrophobic regions. The time interval between two pictures is 0.1 s and the bar corresponds to 1 cm. In order to visualize the track, we put the glass slide on a sheet of paper with shaded regions corresponding to the approximate location of the hydrophobic parts. The dark object appearing in the top two panels is the pipette used to deposit the liquid (and its image by reflection on the glass).

FIG. 7. Photograph of the profile of a large droplet (L = 1.2 cm). The picture is symmetric because of the reflection of the image on the substrate. The arrow indicates the direction of motion.